

Theory of Speciation Transitions in Diffusion Models with General Class Structure

Beatrice Achilli¹, Marco Benedetti¹, Giulio Biroli² and Marc Mézard¹

¹Department of Computing Sciences, Bocconi University, Milan, Italy

²Laboratoire de Physique de l’École Normale Supérieure, ENS, Université PSL, CNRS, Sorbonne Université, Université de Paris, F-75005 Paris, France.

Abstract.

Diffusion Models generate data by reversing a stochastic diffusion process, progressively transforming noise into structured samples drawn from a target distribution. Recent theoretical work has shown that this backward dynamics can undergo sharp qualitative transitions, known as speciation transitions, during which trajectories become dynamically committed to data classes. Existing theoretical analyses, however, are limited to settings where classes are identifiable through first moments, such as mixtures of Gaussians with well-separated means. In this work, we develop a general theory of speciation in diffusion models that applies to arbitrary target distributions admitting well-defined classes. We formalize the notion of class structure through Bayes classification and characterize speciation times in terms of free-entropy difference between classes. This criterion recovers known results in previously studied Gaussian-mixture models, while extending to situations in which classes are not distinguishable by first moments and may instead differ through higher-order or collective features. Our framework also accommodates multiple classes and predicts the existence of successive speciation times associated with increasingly fine-grained class commitment. We illustrate the theory on two analytically tractable examples: mixtures of one-dimensional Ising models at different temperatures and mixtures of zero-mean Gaussians with distinct covariance structures. In the Ising case, we obtain explicit expressions for speciation times by mapping the problem onto a random-field Ising model and solving it via the replica method. Our results provide a unified and broadly applicable description of speciation transitions in diffusion-based generative models.

1. Introduction

Since their introduction in the Machine Learning framework, Diffusion Models (DMs) [Sohl-Dickstein et al., 2015, Ho et al., 2020] have established themselves as the state-of-the-art tool for image and video generation [Cui et al., 2023, Chen et al., 2023, Albergo et al., 2025]. Diffusion Models sample their target probability distribution through a denoising procedure. Assume that data are N -dimensional variables distributed according to a probability law $P(a)$. Samples from $P(a)$ can be obtained by initializing a N -dimensional vector to iid standard Gaussian entries, and follow the so called *backward diffusion process*, defined by the stochastic differential equation

$$-dy_t = y_t dt + 2\mathcal{S}(y_t, t)dt + \sqrt{2}d\tilde{W}_t. \quad (1)$$

where $d\tilde{W}_t$ is a Wiener process, and the drift term $\mathcal{S}(y_t, t)$, called score function, is what guarantees that at $t = 0$ we sample from the target distribution $P(a)$. Its exact expression is $\mathcal{S}(x_t, t) = \nabla_x \log P_t(x_t)$, where

$$P_t(x_t) = \int da P(a) \frac{1}{(2\pi\Delta_t)^{\frac{N}{2}}} \exp\left(-\frac{(x - ae^{-t})^2}{2\Delta_t}\right) \quad (2)$$

is the probability distribution of a noise corrupted sample, obtained by sampling $a \sim P(a)$ at $t = 0$ and following until time t the *forward diffusion* Ornstein-Uhlenbeck process

$$dx_t = -x_t dt + \sqrt{2}dW_t. \quad (3)$$

A recent research line aims to characterize theoretically sharp transitions in the qualitative behavior of trajectories during the backward process. Such Symmetry Breaking events [Raya and Ambrogioni, 2023, Biroli et al., 2024, Ambrogioni, 2025, Sclocchi et al., 2025, Behjoo and Chertkov, 2025] were named speciation transitions. They can be illustrated by the following example. Consider an image dataset comprising photos of cats, dogs, eagles and seagulls. At any instant of the backward process, one can try to guess which of the four types of animals will be represented in the final image, at $t = 0$. At the beginning of the backward process, the image is just Gaussian noise, and it is impossible to attribute it to any of the four categories. As backward diffusion proceeds, features from the target distribution gradually emerge, and one is able to guess the final image better than random. Over time, the prediction for a given single trajectory will change, even back and forth, between classes, but well established time windows exist, during which such fluctuations happen only

between a subset of the classes. In our example, there will be a time window during which the prediction fluctuates between cat and dog, but never to a bird, or conversely, between seagull and eagle, but never to a quadruped. The boundaries of such time windows are called *speciation times*. After each speciation, backward trajectories become committed to a smaller subset of classes in the dataset. Conversely, during the forward diffusion process, these transitions mark moments when it becomes hard to guess which class generated the image, now corrupted by increasing amounts of noise.

The timescale of the first speciation transition, separating a first regime, where backward trajectories are purely noisy, and a second one, when features of the data distribution start to emerge, is computed in Biroli et al. [2024], where a spectral criterion is derived. For data coming from a mixture of two Gaussians with different means (separated by a distance of the order \sqrt{N}), they have obtained a speciation time $t_S = \frac{1}{2} \log N$. The extension to more than two Gaussians, and multiple speciation times was discussed in Pavasovic et al. [2025]. The methods adopted in these works have one main limitation: they apply only to target probability distributions where data comes from spatially well separated classes identifiable by the first moments of the associated probability distributions.

In this work we extend the treatment of speciation to a more general setting which only requires that there exist well-defined classes, i.e. that one can assign a typical configuration to a given class almost surely. In order to do that, we give a precise definition, based on the concept of Bayes classifiers, for decomposing a target probability distribution into classes. Then, we introduce a criterion to identify speciation times based on the error probability of a Bayes classifier used to infer the component of origin of a forward diffused data point. This general criterion recovers the previous theory, but it also allows to study more general cases in which the existence of well-defined classes is not identifiable by first moments. Moreover, within this general framework, we also analyze the case of multiple classes leading to several speciation times.

To illustrate the method, we will use as prototypical models first a mixture of 1D Ising models with different temperatures and then a mixture of Gaussians with zero means and different covariances. Interestingly, we are able to obtain analytical expressions for the speciation times in the 1D Ising mixture by mapping the problem into a 1D Ising model with random field, following the replica calculation in [Weigt and Monasson, 1996, Lucibello et al., 2014].

2. Bayes attribution and pure densities mixtures

We are interested in studying probability distributions whose samples can be labeled as belonging to one among a number R of “well distinguished” classes, or components. To model this, we will assume that

$$P(a) = \sum_{r=1}^R w_r P_r(a), \quad (4)$$

where w_r are non-negative weights with $\sum_r w_r = 1$, and $P_r(a)$ represent the different components. Each sample will be assigned to a class s on the basis of the *Bayesian attribution to component*: given a sample a drawn from $P(a)$, we compute

$$P(s | a) = \frac{P(s, a)}{P(a)} = \frac{w_s P_s(a)}{P(a)}, \quad (5)$$

and we assign it to class $\text{argmax } P(s | a)$. Given $P(a)$, there are many ways to decompose it in classes. To address this ambiguity, we shall restrict our analysis to *Proper Density Decompositions*, requiring that, as N increases, the Bayesian Classifier is able to attribute a typical noise-corrupted sample from $P(a)$ with certainty to one of the components of $P(a)$, for any small but finite amount of noise. Formally, let $\tilde{a}_r = a_r + \eta \mathcal{N}(0, \mathbb{I})$ be the random variable obtained by adding i.i.d. Gaussian noise to each feature of a_r , sampled from $P_r(a_r)$. We will say that Eq. (4) forms a *Proper Density Decomposition* of $P(a)$ if, for any r and $s \neq r$, there exists $\eta = O_N(1)$ and $\epsilon(N) = o_N(1)$ such that $P(s | \tilde{a}_r) \leq \epsilon(N)$ with high probability (w.h.p.) over the statistics of \tilde{a}_r .

The property above is a form of concentration when $N \rightarrow \infty$. In the following, we assume that it results from a large deviation form of the probability distribution which is the one that naturally emerges in statistical physics and, also, several high-dimensional problems: assuming $a_r \sim P_r$, then the numbers $P_s(a_r)$, $s = 1, \dots, n$ are random variables, and they can be expressed as $P_s(a) = e^{N f_s(a, N)}$, where $f_s(a, N) = (1/N) \log P_s(a)$. If $N f_s(a_s, N) \gg N f_r(a_s, N)$ w.h.p. over the sampling of a_s for any $r \neq s$ as $N \rightarrow \infty$, we have a *Proper Density Decomposition*. If Eq. (4) is a *Proper Density Decomposition* and the distribution of $f_s(a_r, N)$ concentrates at large N towards its mean, will say that forms a *Pure Density Decomposition*. In that case, one can write

$$P_s(a_r) = e^{N f_{rs} + o(N)}, \quad f_{rs} = \frac{1}{N} \langle \log P_s(a_r) \rangle_{a_r}, \quad (6)$$

where the average is taken over the distribution of diffused samples that originate from component r , and the $o(N)$ contribution encapsulates the dependence on the specific realization of the disorder a_r . This self-averaging

property of $f_s(a_r, N)$ does not hold, for example, when any of the $P_r(a)$ can itself be properly decomposed. In this sense, self-averaging is a signature of a “minimal” proper decomposition of the measure. The concept of pure densities has also been introduced in Biroli and Mézard [2024].

3. General criterion for speciation

Given a Proper Density Decomposition $P(a) = \sum_{r=1}^R w_r P_r(a)$, as defined in Sec. 2, we need a rigorous notion of attribution to a component of a forward-diffused data point x . The most natural way is generalizing *Bayesian attribution to component* to the noise corrupted sample, namely we compute

$$P(s | x; t) = \frac{P(s, x; t)}{P(x; t)} = \frac{w_s P_s(x; t)}{P(x; t)}, \quad (7)$$

where $P(x; t) = \sum_s w_s P_s(x; t)$ and

$$P_s(x; t) = \int d^N a P_s(a) \exp\left(-\frac{(x - ae^{-t})^2}{2\Delta_t}\right), \quad (8)$$

and we assign it to class $\text{argmax } P(s | x; t)$. We say that r and $s \neq r$ are well distinguishable classes at time t if $\epsilon(N) = o_N(1)$ exists, such that $P(s | x; t) \leq \epsilon(N)$ w.h.p. over the statistics of x , obtained by sampling a from $P_r(a)$ and diffusing forward for time t . Otherwise, $P_r(x; t)$ and $P_s(x; t)$ are both finite w.h.p., and we say that class r is merged with class s at time t . When x is obtained by diffusing a sample originated from component r , each of the $P_s(x; t)$ is reminiscent of the partition function of a disordered system. Disorder is represented by the external field x . It is then natural to write

$$P_s(x; t) = e^{N f_{rs}(t) + \delta f_{rs}(x, t)}, \quad f_{rs}(t) = \frac{1}{N} \langle \log P_s(x; t) \rangle_r \quad (9)$$

where the average is taken over the distribution of diffused samples that originate from component r , and the $f_{rs}(x, t) = o(N)$ contribution encapsulates the dependence on the specific realization of the disorder x . Component r can be reliably identified by the Bayesian Classifier as the origin of the trajectory as long as

$$N f_{ss}(t) + \delta f_{ss}(x, t) \gg N f_{rs}(t) + \delta f_{rs}(x, t) \quad \forall s \neq r \quad (10)$$

w.h.p. over the statistics of x . When this condition is not met, component r is merged at time t with component s . Hence, two things happen at once: the Bayes Classifier starts assigning finite probability to more than one class, and with finite probability $\text{argmax } P(s | x; t)$ misattribution the origin of the trajectory. From Eq. (10), one can see that merging occurs when the difference between average free energies becomes comparable with their fluctuations, marking the speciation time t_{rs} .

$$|f_{rr}(t_{rs}) - f_{rs}(t_{rs})| = K \cdot \sqrt{\text{Var}\left[\frac{1}{N} \log P_r(x; t_{rs}) - \frac{1}{N} \log P_s(x; t_{rs})\right]}. \quad (11)$$

The arbitrary constant K is related to how stringent we are in requiring that no misattributions happen between components that are not yet merged. Notice that this criterion involves only the two components whose speciation time we are predicting, regardless of how many components coexist in the target probability distribution. The presence of other components is irrelevant as far as speciation is concerned. As we will see, on the timescale of merging, the difference between the average free energies becomes $O_N(1)$ w.h.p..

3.1. Large N behavior of speciation time

Starting from Eq. (11) one can derive the expected scaling for the speciation time. As we will see, speciation times diverge as $\log N$ in the large N limit. This allows to simplify the computation of both sides in Eq. (11), in terms of an expansion in e^{-2t} . Explicitly, the average free entropy difference reads

$$f_{rr}(t) - f_{rs}(t) = \frac{1}{N} \left[\int dx P_r(x; t) \log P_r(x; t) - \int dx P_r(x; t) \log P_s(x; t) \right]. \quad (12)$$

Notice that this can be seen as the Kullback-Leibler divergence between the components P_r and P_s of the mixture. At large forward times one can approximate $P_r(x; t)$ by expanding in e^{-2t} its exact expression. The result is a Gaussian distribution (see e.g. Biroli et al. [2024]) with mean μ_s and variance Σ_s . Then, the asymptotic average free entropy difference is a Kullback-Leibler divergence between Gaussians

$$D_{\text{KL}}(\mathcal{N}(\mu_r, \Sigma_r) \| \mathcal{N}(\mu_s, \Sigma_s)) = \frac{a_{rs}}{2} (e^{-2t} + e^{-4t}) + \frac{C_{rs}}{4} e^{-4t} + e^{-4t} S_{rs} \quad (13)$$

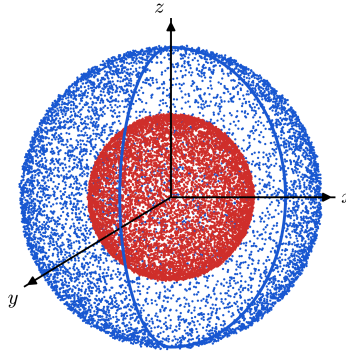


Figure 1: Points scattered on two concentric sphere offer an example of a Pure Density Decomposition, where the two components cannot be distinguished on the basis of their mean.

The values of μ_r , Σ_r , a_{rs} and C_{rs} are simple functions of the first and second moments of the $P_s(x; t = 0)$ distributions. In particular, a_{rs} and C_{rs} are zero if the components have the same mean (see Appendix A for details). Leveraging the Gaussian approximation for $P_r(x; t)$ at large t , one can also approximate the rhs of Eq. (11):

$$\text{Var} \left[\frac{1}{N} \log P_r(x; t) - \frac{1}{N} \log P_s(x; t) \right] = \frac{a_{rs}}{N} (e^{-2t} + 2e^{-4t}) + \frac{C_{rs}}{2N} e^{-4t} + o(e^{-4t}). \quad (14)$$

In this large t regime, leveraging Eqs. (11), (13) and (14) the criterion for speciation reads

(i) If $a_{rs} \neq 0$, i.e. there is separation of first moments,

$$\frac{a_{rs}}{2} e^{-2t} = K \cdot \sqrt{\frac{a_{rs}}{N}} e^{-t} \implies t_{rs} = \frac{1}{2} \log N - \frac{1}{2} \log \left(\frac{4}{a_{rs}} \right) - \log K. \quad (15)$$

This recovers the speciation time scaling obtained in Biroli et al. [2024].

(ii) If $a_{rs} = 0$,

$$\frac{C_{rs}}{4} e^{-4t} = K \cdot \sqrt{\frac{C_{rs}}{2N}} e^{-2t} \implies t_{rs} = \frac{1}{4} \log N - \frac{1}{4} \log \left(\frac{8}{C_{rs}} \right) - \frac{\log K}{2}. \quad (16)$$

This result extends previous results on speciation time to the cases where the class distribution do not have any first moment.

Figure 1 offers an example of a Pure Density Decomposition, where the two components cannot be distinguished on the basis of their mean. Eq. (15) and Eq. (16) show that the arbitrary constant K performs a shift in the speciation time estimates, irrespective of the target measure. Notice that the leading behavior of the speciation times at large N is independent on the details of the target measure. On the other hand, the finite corrections separating speciation times within components of a given target distribution depend on the specific target distribution, and on the specific components under consideration, through a_{rs} and C_{rs} . In both cases, on the timescale of speciations the free entropy differences are $f_{rr}(t_{rs}) - f_{rs}(t_{rs}) = O(1/N)$.

4. Two simple examples: high dimensional Gaussian data

In this section we illustrate our speciation time predictions on two simple target probability distributions. For this examples, we can derive speciation time independently of our criterion by analyzing the explicit transition in the shape of the diffusive potential. We first present a case with first moments separation, namely a mixture of two Gaussians with separate means, which has been analyzed in Biroli et al. [2024]. Then we proceed to a case without first moments separation, namely again a mixture of two Gaussians centered in zero, with different variances. In both settings, the speciation times obtained from the potential argument agree with the scalings reported in Sec. 3.1.

4.1. Gaussian Mixture with different means

Consider a balanced mixture of two multivariate Gaussians with means $\pm m$ and the same isotropic variance σ^2

$$P_t(x) = \frac{1}{2} \frac{1}{(2\pi\Gamma_t)^{N/2}} e^{-\frac{\|x-m e^{-t}\|^2}{2\Gamma_t}} + \frac{1}{2} \frac{1}{(2\pi\Gamma_t)^{N/2}} e^{-\frac{\|x+m e^{-t}\|^2}{2\Gamma_t}}, \quad (17)$$

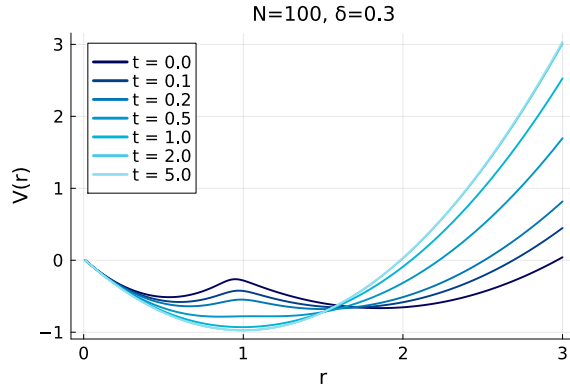


Figure 2: Potential of the reverse SDE as a function of r for different times for a mixture of two Gaussians with zero means and different isotropic variances $\sigma_{1,2}^2 = 1 \pm \delta$. It is clearly noticeable a change in shape, from a single well for large t to a double well for small t . We identify the speciation time in correspondence with the change in curvature in $r = 1$.

where $\Gamma_t = \sigma^2 e^{-2t} + (1 - e^{-2t})$, and assume $\|m\|^2 = N\tilde{\mu}^2$ so that in large dimensions they are well separated. This setting enters the case $a_{rs} \neq 0$, for which our criterion predicts a speciation time $t \sim 1/2 \log N$. We can verify this by looking at the diffusive potential. This was previously done in Biroli et al. [2024], we include it here for completeness. The score function reads

$$S_t(x) = -\frac{x}{\Gamma_t} + m \frac{e^{-t}}{\Gamma_t} \tanh\left(x \cdot m \frac{e^{-t}}{\Gamma_t}\right). \quad (18)$$

The reverse-time backward diffusion process for $x_t \in \mathbb{R}^N$ is the Ornstein-Uhlenbeck process:

$$dx = (x + 2S_t(x)) dt + \sqrt{2}dW_t \quad (19)$$

where dW_t is standard Brownian motion. Introducing the overlap $q(t) = \frac{1}{\sqrt{N}}m \cdot x_t$, we can obtain a closed backward stochastic equation, defined by the potential

$$V(q, t) = \frac{1}{2}q^2 - 2\tilde{\mu}^2 \log \cosh\left(qe^{-t}\sqrt{N}\right) \quad (20)$$

This potential shows a transition: it is quadratic for large times, then at $t = \frac{1}{2} \log N$ it develops a double well structure.

4.2. Gaussian Mixture with different variances

In this section, we study the case of a 2-Gaussians mixture in \mathbb{R}^N , both centered in 0, with different isotropic variances σ_1^2 and σ_2^2 . This setting reproduces the case of $a_{rs} = 0$, for which the scaling of speciation time predicted by our criterion is $t \sim 1/4 \log N$, reported in Eq. 16. The distribution of the mixture at time t is

$$P_t(x) = \frac{1}{2} \frac{1}{(2\pi\Gamma_1)^{N/2}} e^{-\frac{\|x\|^2}{2\Gamma_1}} + \frac{1}{2} \frac{1}{(2\pi\Gamma_2)^{N/2}} e^{-\frac{\|x\|^2}{2\Gamma_2}}, \quad (21)$$

where $\Gamma_{1,2}(t) = \sigma_{1,2}^2 e^{-2t} + (1 - e^{-2t})$. For large N , the target probability density concentrates on thin shells of different radii depending on the two variances. We then choose $\sigma_1^2 = 1 - \delta$ and $\sigma_2^2 = 1 + \delta$, so $\Gamma_1(t) = 1 - \delta e^{-2t}$ and $\Gamma_2(t) = 1 + \delta e^{-2t}$, and tune the parameter $\delta > 0$ in order to have two well distinct radii. The exact score function for this model is $S_t(x) = -\lambda(\|x\|, t)x$, where

$$\lambda(\|x\|, t) = \frac{\Gamma_1^{-N/2} e^{-\|x\|^2/(2\Gamma_1)}/\Gamma_1 + \Gamma_2^{-N/2} e^{-\|x\|^2/(2\Gamma_2)}/\Gamma_2}{\Gamma_1^{-N/2} e^{-\|x\|^2/(2\Gamma_1)} + \Gamma_2^{-N/2} e^{-\|x\|^2/(2\Gamma_2)}}, \quad (22)$$

see Appendix B for details. The reverse-time backward diffusion process for $x_t \in \mathbb{R}^N$ is again the Ornstein-Uhlenbeck process. Introduce the scalar variable $r_t = \frac{\|x_t\|^2}{N}$, the reverse SDE for the radial coordinate reads

$$dr = \left[2(r + 1) - 4r\lambda(\sqrt{Nr}, t) \right] dt + 2\sqrt{\frac{2r}{N}} dB_t = -\frac{\partial V_t(r)}{\partial r} dt + 2\sqrt{\frac{2r}{N}} dB_t, \quad (23)$$

where we have defined the effective potential $V_t(r)$ associated with the deterministic part of the SDE as minus the integral of the drift.

$$V_t(r) = - \int_0^r \left[2(s+1) - 4s\lambda(\sqrt{Ns}, t) \right] ds \quad (24)$$

In Fig. 2, we can see how the shape of the potential evolves in time. One sees a symmetry-breaking phenomenon, from which one can estimate the speciation time for this model. Indeed, we identify the transition as the time where the curvature vanishes in $r = 1$: $\frac{\partial^2 V_t(r=1)}{\partial r^2} = 0$. Thus, we can derive a scaling for the speciation time by imposing that the derivative of $V_t(r)$ is zero at $r = 1$, which translates into $4 - 4\lambda(\sqrt{N}, t_s) = 0$, or more simply

$$\lambda(\sqrt{N}, t_s) = 1. \quad (25)$$

In Appendix B.4 we verify that this condition is indeed satisfied for the desired scaling $t_s \sim \frac{1}{4} \log N$.

5. Speciation times for multi-classes target distributions: 1D Ising mixtures

The aim of this section is to go beyond the toy model presented in the previous section, and focus on a structured high-dimensional probability distribution which leads to well-defined classes that cannot be identified from the first moments.

We consider as target distribution a mixture of 1D Ising models at different inverse temperatures

$$P(\sigma) = \sum_r w_r \frac{1}{Z(\beta_r)} e^{\beta_r \sum_i \sigma_i \sigma_{i+1}}. \quad (26)$$

For large number of spins the different components of the probability distributions are peaked on different regions on the configuration space. However, first moments are identically zero at any β for any component.

This example also showcases how our speciation criterion can be applied to the prediction of all speciation times, in the case of an arbitrary number of components. When the number of components is $n > 2$, our method pinpoints a number of speciation transitions, of which only the first would have been otherwise computable. Notice that, similarly to the described in Sec. 4.2, the components are not spatially well separated; the order parameter in this case is linked to the correlation length. Unlike the Gaussian mixture case, we cannot derive speciation explicitly from the potential. Thus, the general criterion of Eq. (11) becomes essential to predict when components merge. The Bayes attribution to component r of a forward diffused sample x_t reads in this case

$$P(s | x_t) = \frac{P(s) \sum_{\sigma} P(x_t | \sigma) P(\sigma | s)}{P(x_t)} = \frac{\frac{w_s}{Z(\beta_s)} \sum_{\sigma} e^{\sum_i \frac{e^{-t}}{\Delta t} x_i^t \sigma_i + \beta_s \sum_i \sigma_i \sigma_{i+1}}}{\sum_c \frac{w_c}{Z(\beta_c)} \sum_{\sigma} e^{\sum_i \frac{e^{-t}}{\Delta t} x_i^t \sigma_i + \beta_c \sum_i \sigma_i \sigma_{i+1}}} \quad (27)$$

The numerator is the partition function of a 1D Ising spin system at temperature β_r , subject to a (random) external field x_t . According to our criterion, speciations are marked by average difference between pairs of free energies

$$f_s(x, t) = \frac{1}{N} \log \left(\frac{1}{Z(\beta_s)} \sum_{\sigma} e^{\beta_s \sum_{i=1}^{N-1} \sigma_i \sigma_{i+1} + \frac{e^{-t}}{\Delta t} \sum_{i=1}^{N-1} x_i \sigma_i} \right) \quad (28)$$

becoming comparable with their fluctuations, when x_t is generated by sampling a data point a according to one of the P_r , and diffusing it forward in time. Even for relatively low values of N , one can obtain accurate speciation times by using the exact analytical expression for the average free energies and approximation Eq. (14) for the variance. The exact expression for the average free energies is derived in Appendix C.2 making use of replica computations, following the approach reported in Weigt and Monasson [1996]. The main difference is that in our case the individual features of the disorder $(x_t)_i$ are correlated, not i.i.d. variables. The values of C_{rs} can be computed as shown in Appendix C.3

$$C_{rs} = 2 \left[\frac{\tanh^2(\beta_r)}{1 - \tanh^2(\beta_r)} + \frac{\tanh^2(\beta_s)}{1 - \tanh^2(\beta_s)} - \frac{2 \tanh(\beta_r) \tanh(\beta_s)}{1 - \tanh(\beta_r) \tanh(\beta_s)} \right]. \quad (29)$$

The speciation criterion reads

$$|f_{rr}(t_{rs}) - f_{rs}(t_{rs})| = K \sqrt{\frac{C_{rs}}{2N}} e^{-2t_{rs}}. \quad (30)$$

Predicted speciation times will be compared to dynamical ones, defined experimentally in terms of U-turn experiments as follows: sample an initial data a from one of the P_r , and diffuse it forward to x , at time t . Then reverse the process, doing a “U-turn”: start the backward process at time t from x , and follow score-guided

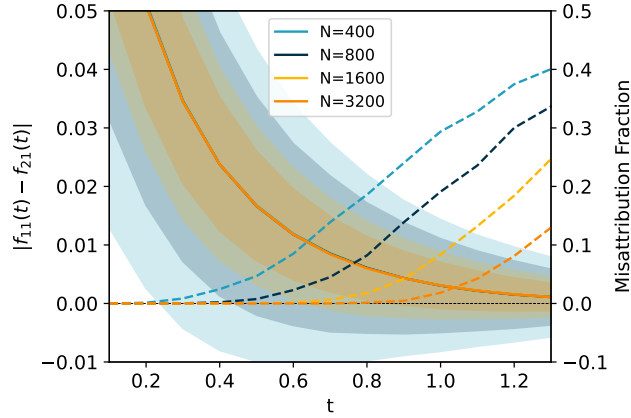


Figure 3: Analysis of a mixture of two 1D Ising models, at inverse temperatures $\beta_1 = 0.5$, $\beta_2 = 1$. Solid lines show the average free entropy difference for different number of spins N as a function of forward diffusion time. The shading represents the 3σ confidence interval. Dashed lines show the misattribution fraction during the forward process. Misattribution starts to rise when zero enters the confidence interval.

diffusion Eq. (19) for a time $t' = t$, reaching b . The score (which can be computed using the transfer matrix method, see Appendix C.5), ensures that b is distributed according to Eq. (4). We then assign b to component s , by means of Bayes attribution. Repeating this experiment many times, one can monitor the probability that b is found in component s knowing that the initial condition a was in component r . Misattribution probability remain very small until $t < t_{rs}$, and it grows when U-turn time surpasses speciation time.

5.1. 2-Ising Mixture

We begin by considering a mixture of two 1D Ising models with $\beta_1 = 0.5$ and $\beta_2 = 1.0$ and $w_1 = w_2 = 0.5$. In Fig. 3 we plot $f_{11} - f_{21}$ during the forward process (solid line) and three times free entropy difference variance as shading, for different number of spins. Dashed lines show empirical misattribution fractions for various N values as a function of U-turn time, in the same color-coding. Empirical misattribution fractions are measured generating 10^4 independent samples from each component, performing a U-turn and measuring the probability that the reconstructed data point is attributed to the same class as its origin. One can notice that when fluctuations of the free entropies difference cross zero, the misattribution fraction starts to rise. Thus, we have an empirical confirmation that our criterion of Eq. (11) captures the correct phenomenon: when the average free entropy difference is of the same order of its fluctuations, setting $K = 3$, we find a misattribution probability of around 1%.

5.2. n -Ising Mixture

In this section, we consider mixtures of more than two Ising chains, showcasing how our theory can predict multiple speciation events. For an easy visual comparison between analytical speciation times and experimental attribution matrices (defined below) we set the constant $K = 1$ in Eq. (30), corresponding to a misattribution fraction $\sim 15\%$.

We start by considering a mixture of 3 Ising models with $\beta_1 = 0.2$, $\beta_2 = 0.3$, and $\beta_3 = 1.0$ and $w_1 = w_2 = w_3 = 1/3$. Sampling starting configurations from the mixture, we perform U-turn experiments at different times, and compute the probability of attributing the spin configuration reconstructed at the end of the backward process to any component. The resulting matrices are displayed in Fig. 4, where the vertical

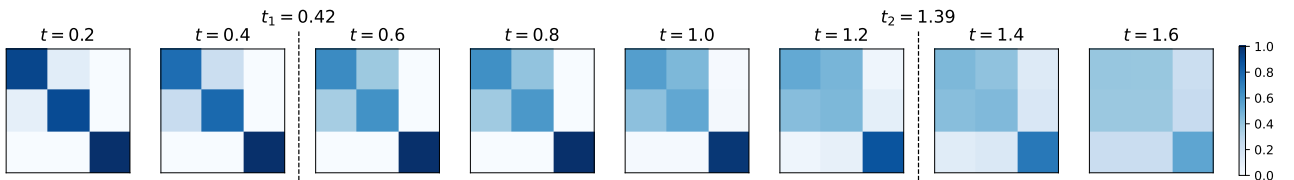


Figure 4: Attribution matrices at the end of the backward process for increasing U-turn times computed numerically with the transfer matrix method. Merging times predicted by our criterion are $t_1 \simeq 0.42$ for inverse temperatures β_1 and β_2 , and $t_2 = 1.39$, for β_2 and β_3 . The target distribution is a 3-Ising mixture with $\beta_1 = 0.2$, $\beta_2 = 0.3$, $\beta_3 = 1.0$; $N = 1600$.

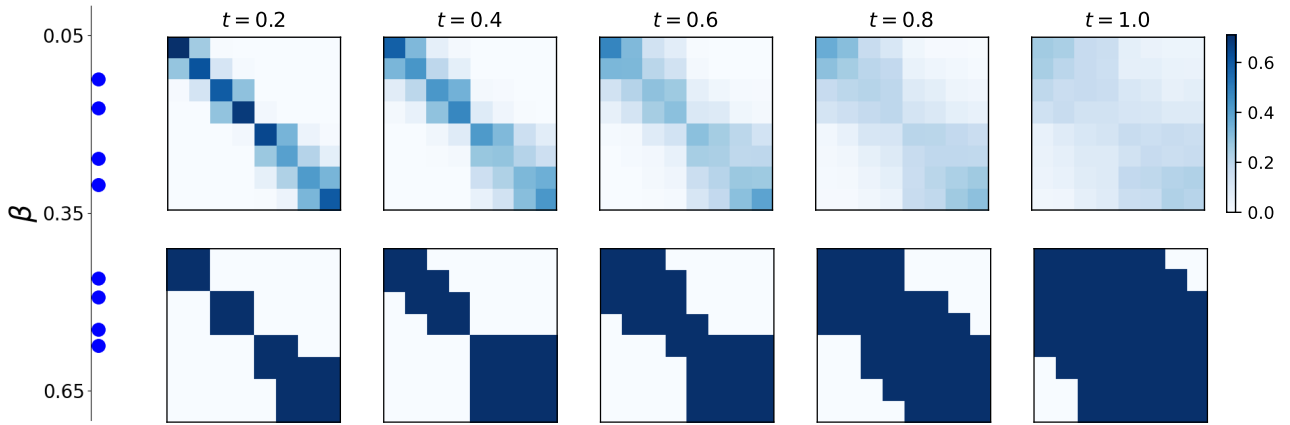


Figure 5: Attribution matrices at the end of the backward process for increasing U-turn times, computed numerically with the transfer matrix method (top row) compared with the analytical ones (bottom row). The target distribution is a 8-Ising mixture with hierarchically generated temperatures (beta values displayed on the left). System size is $N = 1600$.

dimension represents the origin component and the horizontal dimension represents the attribution component. Merging times predicted by our criterion are $t_1 \simeq 0.42$ for inverse temperatures β_1 and β_2 , and $t_2 = 1.39$, for β_2 and β_3 (and, consequently, also β_1 and β_3 since the first two components were already merged). Notice how two values of β are quite similar, leading to a short merging time. The empirical attribution matrices are almost diagonal for small t_U . As time increases, and in particular after passing the predicted merging times, the block structure in the attribution matrices is revealed.

Next, we consider a homogeneous mixture of 8 Ising chains with hierarchically organized inverse temperatures (β values displayed in Fig. 5). We perform again the U-turn experiment and obtain empirical the attribution matrices (top row). Empirical results are then compared with a matrix representation of the analytical predictions (bottom row), where blocks are colored if $|f_{rr}(t_{rs}) - f_{rs}(t_{rs})| < \sqrt{\frac{C_{rs}}{2N}} e^{-2t_{rs}}$. There is good agreement between attribution matrices obtained analytically and numerically for all the U-turn times considered. The emerging block structure can again be explained with subsequent speciation events, where backwards trajectories commit to a smaller and smaller set of temperatures, and finally to a specific temperature.

6. Conclusions

In this work, we have extended the theoretical understanding of speciation transitions in generative diffusion models to the case of data originating from mixture distributions, where components are peaked on different regions which cannot simply be identified by first moments. We have done so by introducing a new criterion for speciation, based on the analysis of the Bayes component attribution during the forward process, and free-entropy differences. The important outcome of our analysis is that merging times between different components scale logarithmically with the dimension of the sample space, and are separated by finite time gaps, giving rise to a hierarchical structure of attribution.

As a practical example, we applied the technique to mixtures of 1D Ising models, deriving explicit expressions for the mean and variance of the free entropy difference between components as a function of time. Our analysis reveals that both the mean and the standard deviation of this difference decay exponentially with time, and that the critical timescale for speciation is logarithmic in the system size, $t_S \sim \frac{1}{4} \log N$. We have validated our theoretical predictions with numerical experiments, demonstrating excellent agreement between analytical and empirical results for the onset of misattribution between components. Our approach provides a principled criterion for speciation, that is applicable to a wide range of mixture statistical physics models, as long as each component has finite correlation length.

These findings contribute to the growing theoretical foundation of diffusion models and highlight the universality of the speciation phenomenon in high-dimensional generative processes.

Acknowledgments GB was supported by ANR PRAIRIE-PSAI (France 2023) « ANR-23-IACL-0008 ».

References

Michael S. Albergo, Nicholas M. Boffi, and Eric Vanden-Eijnden. Stochastic Interpolants: A Unifying Framework for Flows and Diffusions, October 2025.

Luca Ambrogioni. The Statistical Thermodynamics of Generative Diffusion Models: Phase Transitions, Symmetry Breaking, and Critical Instability. *Entropy*, 27(3):291, March 2025. ISSN 1099-4300. doi: 10.3390/e27030291.

Hamidreza Behjoo and Michael Chertkov. U-Turn Diffusion. *Entropy*, 27(4):343, April 2025. ISSN 1099-4300. doi: 10.3390/e27040343.

Giulio Biroli and Marc Mézard. Kernel density estimators in large dimensions. *arXiv:2408.05807*, 2024.

Giulio Biroli, Tony Bonnaire, Valentin de Bortoli, and Marc Mézard. Dynamical regimes of diffusion models. *Nature Communications*, 15(1):9957, 2024. ISSN 2041-1723.

Sitan Chen, Sinho Chewi, Jerry Li, Yuanzhi Li, Adil Salim, and Anru R. Zhang. Sampling is as easy as learning the score: Theory for diffusion models with minimal data assumptions, April 2023.

Hugo Cui, Florent Krzakala, Eric Vanden-Eijnden, and Lenka Zdeborova. Analysis of Learning a Flow-based Generative Model from Limited Sample Complexity. In *The Twelfth International Conference on Learning Representations*, October 2023.

Jonathan Ho, Ajay Jain, and Pieter Abbeel. Denoising diffusion probabilistic models. In *Neural Information Processing Systems*. NeurIPS, 2020.

Carlo Lucibello, Flaviano Morone, and Tommaso Rizzo. One-dimensional disordered ising models by replica and cavity methods. *Physical Review E*, 90(1), July 2014. ISSN 1550-2376. doi: 10.1103/physreve.90.012140.

Krunoslav Lehman Pavasovic, Jakob Verbeek, Giulio Biroli, and Marc Mezard. Classifier-free guidance: From high-dimensional analysis to generalized guidance forms. *arXiv preprint arXiv:2502.07849*, 2025.

Gabriel Raya and Luca Ambrogioni. Spontaneous symmetry breaking in generative diffusion models. In *Thirty-seventh Conference on Neural Information Processing Systems*, 2023.

Antonio Sclocchi, Alessandro Favero, and Matthieu Wyart. A phase transition in diffusion models reveals the hierarchical nature of data. *Proceedings of the National Academy of Sciences*, 122(1):e2408799121, January 2025. doi: 10.1073/pnas.2408799121.

Jascha Sohl-Dickstein, Eric A. Weiss, Niru Maheswaranathan, and Surya Ganguli. Deep unsupervised learning using nonequilibrium thermodynamics. In *International Conference on Machine Learning*. ICML, 2015.

M Weigt and R Monasson. Replica structure of one-dimensional disordered ising models. *Europhysics Letters (EPL)*, 36(3):209–214, October 1996. ISSN 1286-4854. doi: 10.1209/epl/i1996-00212-8.

Appendix A. Large time analysis

Explicitly, the average free entropy difference reads

$$f_{rr}(t) - f_{rs}(t) = \frac{1}{N} \left[\int dx P_r(x; t) \log P_r(x; t) - \int dx P_r(x; t) \log P_s(x; t) \right]. \quad (\text{A.1})$$

Notice that this can be seen as the Kullback-Leibler divergence between the components of the mixture. At large forward times one can obtain $P_r(x; t)$ by expanding in e^{-2t} its exact expression. The result is a Gaussian distribution (see e.g. Biroli et al. [2024])

$$\log P_r(x; t) = \text{const} + \frac{e^{-t}}{\Delta_t} \sum_{i=1}^N x_i \langle a_i \rangle_r - \frac{1}{2\Delta_t} \sum_{i,j=1}^N x_i M_{r,ij} x_j + O((xe^{-t})^3), \quad (\text{A.2})$$

where

$$M_{r,ij} = \delta_{ij} - e^{-2t} (\langle a_i a_j \rangle_r - \langle a_i \rangle_r \langle a_j \rangle_r). \quad (\text{A.3})$$

and $\Delta_t = 1 - e^{-2t}$, so when we expand in e^{-t} we write

$$\frac{1}{\Delta_t} = \frac{1}{1 - e^{-2t}} = 1 + e^{-2t} + e^{-4t} + O(e^{-4t}) \quad \frac{1}{\Delta_t^2} = \frac{1}{(1 - e^{-2t})^2} = 1 + 2e^{-2t} + 3e^{-4t} + O(e^{-4t}) \quad (\text{A.4})$$

Completing the square in (A.2) yields a Gaussian with

$$\mu_r(t) = \frac{e^{-t}}{\Delta_t} M_r^{-1} \langle a \rangle_r = e^{-t} (1 + e^{-2t} + e^{-4t}) [I + e^{-2t} C + O(e^{-4t})] \langle a \rangle_r \quad (\text{A.5})$$

$$= e^{-t} [\langle a \rangle_r + e^{-2t} (\langle a \rangle_r + C_r \langle a \rangle_r) + O(e^{-4t})], \quad (\text{A.6})$$

$$\Sigma_r(t) = \frac{1}{\Delta_t} \Delta_t M_r^{-1} = I + e^{-2t} C_r + O(e^{-4t}), \quad (\text{A.7})$$

where $C_{r,ij} = \langle a_i a_j \rangle_r - \langle a_i \rangle_r \langle a_j \rangle_r$. Then, the average free entropy difference is a Kullback-Leibler divergence between Gaussians

$$D_{\text{KL}}(\mathcal{N}(\mu_r, \Sigma_r) \| \mathcal{N}(\mu_s, \Sigma_s)) = \frac{1}{2} \left[\text{Tr}(\Sigma_s^{-1} \Sigma_r) + (\mu_s - \mu_r)^\top \Sigma_s^{-1} (\mu_s - \mu_r) - N - \log \frac{\det \Sigma_r}{\det \Sigma_s} \right]. \quad (\text{A.8})$$

Define

$$\Delta_{rs} a_i = \langle a_i \rangle_r - \langle a_i \rangle_s, \quad (\text{A.9})$$

$$\Delta_{rs} C_{ij} = (\langle a_i a_j \rangle_r - \langle a_i \rangle_r \langle a_j \rangle_r)_r - (\langle a_i a_j \rangle_s - \langle a_i \rangle_s \langle a_j \rangle_s)_s, \quad (\text{A.10})$$

then using the Gaussian KL formula and expanding up to $O(e^{-4t})$ gives

$$\frac{1}{N} D_{\text{KL}}(P_r(\cdot, t) \| P_s(\cdot, t)) = \frac{1}{2N} \frac{e^{-2t}}{\Delta_t} \sum_i (\Delta_{rs} a_i)^2 + \frac{e^{-4t}}{4N} \frac{1}{\Delta_t^2} \sum_{i,j} (\Delta_{rs} C_{ij})^2 \quad (\text{A.11})$$

$$+ \frac{e^{-4t}}{2N} \frac{1}{\Delta_t} \left[2 \sum_i \Delta_{rs} a_i \left(\sum_j C_{s,ij} \langle a_j \rangle_s - \sum_j C_{r,ij} \langle a_j \rangle_r \right) - \sum_{i,j} \Delta_{rs} a_i C_{s,ij} \Delta_{rs} a_j \right] + O(e^{-4t}). \quad (\text{A.12})$$

Now expand Δ_t and retain terms through $O(e^{-4t})$

$$\frac{1}{N} D_{\text{KL}} = \frac{1}{2N} (e^{-2t} + e^{-4t}) \sum_i (\Delta_{rs} a_i)^2 + \frac{e^{-4t}}{4N} \sum_{i,j} (\Delta_{rs} C_{ij})^2 \quad (\text{A.13})$$

$$+ \frac{e^{-4t}}{2N} \left[2 \sum_i \Delta_{rs} a_i \left(\sum_j C_{ij}^{(s)} \langle a_j \rangle_s - \sum_j C_{ij}^{(r)} \langle a_j \rangle_r \right) - \sum_{i,j} \Delta_{rs} a_i C_{ij}^{(s)} \Delta_{rs} a_j \right] + O(e^{-4t}) \quad (\text{A.14})$$

$$\simeq \frac{a_{rs}}{2} (e^{-2t} + e^{-4t}) + \frac{C_{rs}}{4} e^{-4t} + e^{-4t} S_{rs}, \quad (\text{A.15})$$

where

$$a_{rs} = \frac{\sum_i (\Delta_{rs} a_i)^2}{N}, \quad C_{rs} = \frac{\sum_{i,j} (\Delta_{rs} C_{ij})^2}{N}, \quad (\text{A.16})$$

$$S_{rs} = \frac{2 \sum_i \Delta_{rs} a_i \left(\sum_j C_{s,ij} \langle a_j \rangle_s - \sum_j C_{r,ij} \langle a_j \rangle_r \right) - \sum_{i,j} \Delta_{rs} a_i C_{s,ij} \Delta_{rs} a_j}{2N} \quad (\text{A.17})$$

Leveraging the Gaussian approximation for $P_r(x; t)$ at large t , one can also approximate $\text{Var}[\frac{1}{N} \log P_s(x; t) - \frac{1}{N} \log P_r(x; t)]$. Specifically:

$$\frac{1}{N} \log P_r(x; t) - \frac{1}{N} \log P_s(x; t) = \frac{1}{N} \left[\frac{e^{-t}}{\Delta_t} \sum_i x_i \Delta_{rs} a_i + \frac{e^{-2t}}{2\Delta_t} \sum_{i,j} x_i \Delta_{rs} C_{ij} x_j \right] + O((xe^{-t})^3). \quad (\text{A.18})$$

The dominant contribution to the variance comes from considering $x_i \simeq z_i$ with $z_i \stackrel{\text{i.i.d.}}{\sim} \mathcal{N}(0, 1)$. The linear and quadratic parts are uncorrelated for a centered Gaussian, so

$$\text{Var} \left[\frac{1}{N} \log P_s(x; t) - \frac{1}{N} \log P_r(x; t) \right] = \text{Var} \left[\frac{e^{-t}}{N\Delta_t} \sum_i \Delta_{rs} a_i z_i \right] + \text{Var} \left[\frac{e^{-2t}}{2N\Delta_t} \sum_{i,j} \Delta_{rs} C_{ij} z_i z_j \right] + O(e^{-6t}) \quad (\text{A.19})$$

$$= \frac{e^{-2t}}{N^2} \frac{1}{\Delta_t^2} \sum_i (\Delta_{rs} a_i)^2 + \frac{e^{-4t}}{2N^2} \frac{1}{\Delta_t^2} \sum_{i,j} (\Delta_{rs} C_{ij})^2 + O(e^{-6t}). \quad (\text{A.20})$$

Expanding also Δ_t and keeping through $O(e^{-4t})$,

$$\text{Var} \left[\frac{1}{N} \log P_r(x, t) - \frac{1}{N} \log P_s(x, t) \right] \simeq (e^{-2t} + 2e^{-4t}) \frac{1}{N^2} \sum_i (\Delta_{rs} a_i)^2 + \frac{e^{-4t}}{2N^2} \sum_{i,j} (\Delta_{rs} C_{ij})^2 \quad (\text{A.21})$$

$$\simeq \frac{a_{rs}}{N} (e^{-2t} + 2e^{-4t}) + \frac{C_{rs}}{2N} e^{-4t}. \quad (\text{A.22})$$

In this large t regime, the criterion for speciation then reads

(i) If $a_{rs} \neq 0$,

$$\frac{a_{rs}}{2} e^{-2t} = K \cdot \sqrt{\frac{a_{rs}}{N}} e^{-t} \implies t_{rs} = \frac{1}{2} \log N - \frac{1}{2} \log \left(\frac{4}{a_{rs}} \right) - \log K. \quad (\text{A.23})$$

This recovers the speciation time scaling obtained in Biroli et al. [2024].

(ii) If $a_{rs} = 0$,

$$\frac{C_{rs}}{4} e^{-4t} = K \cdot \sqrt{\frac{C_{rs}}{2N}} e^{-2t} \implies t_{rs} = \frac{1}{4} \log N - \frac{1}{4} \log \left(\frac{8}{C_{rs}} \right) - \frac{\log K}{2}. \quad (\text{A.24})$$

This case extends previous literature on speciation time to cases where the class distribution do not have any first moment.

Notice that, on this timescale, $\text{Var}[1/N \log P_r(x; t) - 1/N \log P_s(x; t)] = O(\frac{1}{N^2})$: this is due to a combination of factors: a free entropy variance has a natural scaling of $1/N$, at fixed time. But speciation happens on a timescale which is logarithmic in N , which contributes an additional $1/N$ factor to the variance. Hence, an equivalent definition of speciation time is $f_{rr}(t) - f_{rs}(t) \simeq 1/N$.

Appendix B. Mixture of Gaussians with different covariance

Appendix B.1. General criterion

For completion, we also compute the speciation time prediction from Eq. (11) for the mixture of Gaussians defined in Eq.(21). The left-hand side is

$$f_{11}(t) - f_{21}(t) = -\frac{1}{2} \left[\log \frac{\Gamma_1(t)}{\Gamma_2(t)} + 1 - \frac{\Gamma_1(t)}{\Gamma_2(t)} \right] \quad (\text{B.1})$$

and the right-hand side

$$\text{Var} \left[\frac{1}{N} \log P_1(x; t) - \frac{1}{N} \log P_2(x; t) \right] = \frac{1}{2N} \Gamma_1(t)^2 \left(\frac{1}{\Gamma_1(t)} - \frac{1}{\Gamma_2(t)} \right)^2. \quad (\text{B.2})$$

The Bayes attribution criterion then reads

$$\frac{1}{2} \left[\log \frac{\Gamma_1(t)}{\Gamma_2(t)} + 1 - \frac{\Gamma_1(t)}{\Gamma_2(t)} \right] = \frac{1}{\sqrt{2N}} \left(1 - \frac{\Gamma_1(t)}{\Gamma_2(t)} \right). \quad (\text{B.3})$$

For our choice of $\Gamma(t)$

$$\frac{\Gamma_1(t)}{\Gamma_2(t)} = \frac{1 - \delta e^{-2t}}{1 + \delta e^{-2t}} \approx 1 - 2\delta e^{-2t} \quad (\text{B.4})$$

so

$$\log(1 - 2\delta e^{-2t}) + 2\delta e^{-2t} \simeq \frac{2\delta e^{-2t}}{\sqrt{2N}} \quad (\text{B.5})$$

and expanding the log we obtain

$$\delta e^{-2t} \simeq \frac{1}{\sqrt{2N}} \quad (\text{B.6})$$

from which $t_s = \frac{1}{4} \log N$.

Appendix B.2. Score function

To compute the exact score function, defined as $S_t(x) = \nabla_x \log p_t(x)$, one can define the weights:

$$w_i(x) = \Gamma_i^{-N/2} e^{-\frac{\|x\|^2}{2\Gamma_i}} \quad (\text{B.7})$$

and call

$$m_i(x) = \frac{w_i(x)}{w_1(x) + w_2(x)}. \quad (\text{B.8})$$

Then, the exact score is:

$$S_t(x) = -x \left(\frac{m_1(x)}{\Gamma_1} + \frac{m_2(x)}{\Gamma_2} \right) \quad (\text{B.9})$$

$$= -\lambda(\|x\|, t)x \quad (\text{B.10})$$

where

$$\lambda(\|x\|, t) = \frac{\Gamma_1^{-N/2} e^{-\|x\|^2/(2\Gamma_1)} / \Gamma_1 + \Gamma_2^{-N/2} e^{-\|x\|^2/(2\Gamma_2)} / \Gamma_2}{\Gamma_1^{-N/2} e^{-\|x\|^2/(2\Gamma_1)} + \Gamma_2^{-N/2} e^{-\|x\|^2/(2\Gamma_2)}} \quad (\text{B.11})$$

Appendix B.3. Radial SDE

We consider the Ornstein-Uhlenbeck reverse-time diffusion process for $x_t \in \mathbb{R}^N$:

$$dx = (x + 2S_t(x)) dt + \sqrt{2}dW_t \quad (\text{B.12})$$

where dW_t is standard Brownian motion. Our goal is to obtain an equation for the speciation time, similarly to what was done in Biroli et al. [2024] for the case of a mixture of Gaussians centered respectively in $\pm m$, with $\|m\|^2 = N\mu$. Define the scalar variable:

$$r_t = \frac{\|x_t\|^2}{N} \quad (\text{B.13})$$

Using Itô's lemma:

$$dr = \frac{2}{N} x^\top dx + \frac{1}{N} \text{Tr}(dx dx^\top) \quad (\text{B.14})$$

From the SDE for x_t we see $dx dx^\top = 2Idt$, so

$$dr = \frac{2}{d} x^\top (x + 2S_t(x)) dt + 2dt + \frac{2\sqrt{2}}{N} x^\top dW_t \quad (\text{B.15})$$

$$= [2r + 4\alpha(t, x) + 2] dt + \frac{2\sqrt{2}}{N} x^\top dW_t \quad (\text{B.16})$$

where $\alpha(t, x) = \frac{1}{N} x^\top S_t(x)$.

Using our expression for the score $S_t(x) = -\lambda(\|x\|, t)x$, we get:

$$\alpha(r, t) = -r\lambda(\sqrt{Nr}, t) \quad (\text{B.17})$$

so the drift becomes:

$$2r + 4\alpha(r, t) + 2 = 2(r + 1) - 4r\lambda(\sqrt{Nr}, t) \quad (\text{B.18})$$

The noise term can be rewritten as

$$\frac{2\sqrt{2}}{N} x^\top dW_t \approx 2\sqrt{\frac{2r}{N}} dB_t \quad (\text{B.19})$$

which is negligible for large N .

Putting all together, we find

$$dr = \left[2(r+1) - 4r\lambda(\sqrt{Nr}, t) \right] dt + 2\sqrt{\frac{2r}{N}} dB_t \quad (\text{B.20})$$

Appendix B.4. Scaling of speciation time

We can verify that the scaling for the speciation time obtained from the change of shape of the potential is the expected one of $t_s \sim 1/4 \log N$. To do so, consider

$$\lambda(\sqrt{N}, t) = \frac{\Gamma_1^{-N/2-1} \exp\left(-\frac{N}{2\Gamma_1}\right) + \Gamma_2^{-N/2-1} \exp\left(-\frac{N}{2\Gamma_2}\right)}{\Gamma_1^{-N/2} \exp\left(-\frac{N}{2\Gamma_1}\right) + \Gamma_2^{-N/2} \exp\left(-\frac{N}{2\Gamma_2}\right)}, \quad (\text{B.21})$$

with

$$\Gamma_1 = 1 - \varepsilon, \quad \Gamma_2 = 1 + \varepsilon, \quad \varepsilon = \delta e^{-2t}. \quad (\text{B.22})$$

We are interested in the scaling $t_s = \frac{1}{4} \log N + b$, so that

$$\varepsilon_s = \delta e^{-2t_s} = \frac{\delta e^{-2b}}{\sqrt{N}} = \frac{a}{\sqrt{N}}, \quad a := \delta e^{-2b}, \quad (\text{B.23})$$

and we write simply $\varepsilon = a/\sqrt{N}$.

Define

$$B_1 = \Gamma_1^{-N/2} \exp\left(-\frac{N}{2\Gamma_1}\right), \quad B_2 = \Gamma_2^{-N/2} \exp\left(-\frac{N}{2\Gamma_2}\right), \quad (\text{B.24})$$

so that $\lambda = \frac{B_1/\Gamma_1 + B_2/\Gamma_2}{B_1 + B_2}$. One can factor out B_1 and set $r = \frac{B_2}{B_1}$, to get

$$\lambda = \frac{\Gamma_1^{-1} + r \Gamma_2^{-1}}{1 + r} = \frac{(1 - \varepsilon)^{-1} + r(1 + \varepsilon)^{-1}}{1 + r}. \quad (\text{B.25})$$

A standard Taylor expansion in ε of r gives $\log r = \frac{2N}{3} \varepsilon^3 + O(N\varepsilon^5)$, and with $\varepsilon = a/\sqrt{N}$ this becomes

$$\Delta = \log r = \frac{2}{3} \frac{a^3}{\sqrt{N}} + O\left(\frac{1}{N^{3/2}}\right). \quad (\text{B.26})$$

Thus $r = e^\Delta = 1 + \Delta + \frac{\Delta^2}{2} + O(\Delta^3)$, and both Δ and ε are of order $N^{-1/2}$.

Using the expansions above and keeping terms up to second order in ε and Δ ,

$$\lambda \simeq \frac{1 + \varepsilon^2 + \frac{\Delta}{2}(1 - \varepsilon) + \frac{\Delta^2}{4}}{1 + \frac{\Delta}{2} + \frac{\Delta^2}{4}}. \quad (\text{B.27})$$

Now expand the ratio for small Δ up to terms of order $O(\varepsilon^2\Delta)$ and $O(\Delta^2)$,

$$\lambda \simeq 1 + \varepsilon^2 - \frac{\Delta\varepsilon}{2} + O\left(\frac{1}{N^{3/2}}\right). \quad (\text{B.28})$$

Finally, we insert the scalings for ε and Δ

$$\lambda(\sqrt{N}, t_s) = 1 + \frac{a^2}{N} - \frac{a^4}{3N} + O\left(\frac{1}{N^{3/2}}\right) = 1 + \frac{a^2\left(1 - \frac{a^2}{3}\right)}{N} + O\left(\frac{1}{N^{3/2}}\right). \quad (\text{B.29})$$

To cancel the $1/N$ term we impose

$$a^2\left(1 - \frac{a^2}{3}\right) = 0, \quad (\text{B.30})$$

which gives the nontrivial solution $a^2 = 3$, i.e. $a = \sqrt{3}$. Since $a = \delta e^{-2b}$, we have

$$\delta e^{-2b} = \sqrt{3} \quad \Rightarrow \quad b = \frac{1}{2} \log \delta - \frac{1}{4} \log 3, \quad (\text{B.31})$$

and thus

$$t_s = \frac{1}{4} \log N + \frac{1}{2} \log \delta - \frac{1}{4} \log 3. \quad (\text{B.32})$$

Appendix C. 1D Ising mixtures

This section details the computation of the score, the empirical free entropy and the average free entropy in the case where $P(a) = \sum_{r=1}^R w_r P_{\beta_r}(a)$ is a mixture of 1D Ising models at different inverse temperatures β_r , where every component of the mixture has the form

$$P_{\beta}(s) = \frac{1}{Z(\beta)} e^{\beta \sum_{i=1}^{N-1} \sigma_i \sigma_{i+1}}, \quad (\text{C.1})$$

where $Z(\beta) = (2 \cosh \beta)^{N-1}$, and $\sum_r w_r = 1$.

Appendix C.1. Bayesian Attribution

The Bayesian probability for a trajectory to have originated from component s given its value x_t is given by

$$P(s | x_t) = \frac{P(s, x_t)}{P(x_t)} = \frac{P(s)P(x_t | s)}{P(x_t)} = \frac{P(s) \sum_{\sigma} P(x_t | \sigma)P(\sigma | s)}{P(x_t)} \quad (\text{C.2})$$

leading to

$$P(s | x_t) = \frac{\frac{w_s}{Z(\beta_s)} \sum_{\sigma} e^{\sum_i \frac{e^{-t}}{\Delta t} x_i^t \sigma_i + \beta_s \sum_i \sigma_i \sigma_{i+1}}}{\sum_c \frac{w_c}{Z(\beta_c)} \sum_{\sigma} e^{\sum_i \frac{e^{-t}}{\Delta t} x_i^t \sigma_i + \beta_c \sum_i \sigma_i \sigma_{i+1}}} \quad (\text{C.3})$$

$$= \frac{w_s e^{N f_s(x, t) - \log Z(\beta_s)}}{\sum_c w_c e^{N P_c(x, t) - \log Z(\beta_c)}} \quad (\text{C.4})$$

where

$$f_s(x, t) = \frac{1}{N} \log \left(\sum_{\sigma} e^{\beta_s \sum_{i=1}^{N-1} \sigma_i \sigma_{i+1} + \frac{e^{-t}}{\Delta t} \sum_{i=1}^{N-1} x_i \sigma_i} \right) \quad (\text{C.5})$$

is the free-entropy of a 1D Ising model with random field $h_i = \frac{e^{-t}}{\Delta t} x_i$. It can be computed using the transfer matrix method.

Appendix C.2. Analytic computation of the average free entropy

Our criterion for speciation prescribes computing the average f_{rs} Eq. (C.5), when x is generated by sampling a data point a according to P_r , and diffusing it forward in time. Then, $x = a e^{-t} + z \sqrt{\Delta t}$ where z is a centered N -dimensional Gaussian random variable with covariance \mathbb{I}_N . We can obtain an exact expression for this quantity, making use of replica computations following the approach reported in Weigt and Monasson [1996]. The main difference is that in our case the noise is partially correlated with the data. Hence

$$f_{rs}(t) = \left\langle \frac{1}{N} \log \left(\sum_{\sigma} e^{\beta_r \sum_{i=1}^{N-1} \sigma_i \sigma_{i+1} + \frac{e^{-t}}{\Delta t} \sum_{i=1}^{N-1} (a_i e^{-t} + z_i \sqrt{\Delta t}) \sigma_i} \right) \right\rangle_{a \sim P_r(a), z} \quad (\text{C.6})$$

We compute this quantity by means of the replica trick, in the Replica Symmetric approximation. First, we need to compute integer powers

$$\langle Z^n \rangle = \left\langle \left(\sum_{\sigma} e^{\beta_r \sum_{i=1}^{N-1} \sigma_i \sigma_{i+1} + \frac{e^{-t}}{\Delta t} \sum_{i=1}^{N-1} (a_i e^{-t} + z_i \sqrt{\Delta t}) \sigma_i} \right)^n \right\rangle_{a \sim P_r(a), z} \quad (\text{C.7})$$

$$= \frac{1}{Z(\beta_r)} \sum_{\sigma^a} e^{\beta_r \sum_i \sigma_i^a \sigma_{i+1}^a + \beta_s \sum_{i,a} \sigma_i^a \sigma_{i+1}^a + \gamma^2 \sum_i \sigma_i^a \sum_a \sigma_i^a \langle \langle e^{\gamma \sum_i z_i \sum_a \sigma_i^a} \rangle \rangle_z}. \quad (\text{C.8})$$

where we defined $\gamma = \frac{e^{-t}}{\sqrt{\Delta t}}$. The n replicas σ^a , $a = 1, \dots, n$ account for the power n , the $n+1$ replica σ^0 accounts for the prior $P_r(a) = \frac{1}{Z(\beta_r)} e^{\beta_r \sum_i a_i a_{i+1}}$, and then make the continuation to real n using the identity

$$f_{rs}(t) = \lim_{n \rightarrow 0} \frac{\langle Z^n \rangle - 1}{n}. \quad (\text{C.9})$$

To describe the replica symmetric subspace we introduce vectors $|\sigma^0, a_1 \dots a_p\rangle$, where we have p spins up at indices a_j . Then, we take the sum of such vectors

$$||\sigma^0, p\rangle\rangle = \sum_{a_1 < \dots < a_p} |\sigma^0, a_1 \dots a_p\rangle \quad (\text{C.10})$$

and the collection of these vectors $|\langle \sigma^0, p \rangle\rangle_{\sigma^0=\pm 1, p=1, \dots, n}$ gives the RS subspace of dimension $2(n+1)$ (see Lucibello et al. [2014] for details). Then, we look at the replicated transfer matrix $T_{2^{n+1} \times 2^{n+1}}$ projected onto this subspace

$$\langle\langle \sigma^0, q | |T| | \tilde{\sigma}^0, p \rangle\rangle = e^{\beta_r \sigma^0 \tilde{\sigma}^0} e^{\gamma^2 \sigma^0 (2q-n)} \langle\langle e^{\gamma z (2q-n)} \rangle\rangle_z \sum_{r=r_{min}}^{r_{max}} \binom{q}{r} \binom{n-q}{p-r} e^{\beta_s (4r-2q-2p+n)} \quad (\text{C.11})$$

with $r_{min} = \max(0, p+q-n)$ and $r_{max} = \min(p, q)$. The site-dependent partition function in the RS approximation is given by

$$Z_{i+1}(\tilde{\sigma}^0, p) = \sum_{\sigma^0=\pm 1} \sum_{q=0}^n T(\sigma^0, q; \sigma^0, p) Z_i(\sigma^0, q). \quad (\text{C.12})$$

We can write this in a function basis, defining $Z_i^{\sigma^0}[x] = \sum_{p=0}^n Z_i(\sigma^0, p) x^p$. Equation (C.12) now reads

$$Z_{i+1}^{\tilde{\sigma}^0}[x] = \int_0^\infty \sum_{\sigma^0=\pm 1} e^{\beta_r \sigma^0 \tilde{\sigma}^0} K_n^{\sigma^0}(x, y) Z_i^{\sigma^0}[y] dy \quad (\text{C.13})$$

where the kernel $K_n^{\sigma^0}(x, y) = e^{\beta_s n} (1 + xe^{-2\beta_s})^n e^{-\gamma^2 \sigma^0 n} \langle\langle \delta(y - g^{\sigma^0}(x, z)) e^{-n\gamma z} \rangle\rangle_z$ is the representation of the transfer matrix in the space of polynomials, and

$$g^{\sigma^0}(x, z) = e^{2\gamma z} \frac{e^{-\beta_s} + xe^{\beta_s}}{e^{\beta_s} + xe^{-\beta_s}} e^{2\gamma^2 \sigma^0}. \quad (\text{C.14})$$

As we are interested in the behavior of the largest eigenvalue of the transfer matrix kernel in the limit $n \rightarrow 0$, we focus on the eigenvectors with largest eigenvalue of the $n = 0$ kernel

$$K = \begin{pmatrix} \frac{e^{\beta_r}}{2 \cosh \beta_r} K^+(x, y) & \frac{e^{-\beta_r}}{2 \cosh \beta_r} K^-(x, y) \\ \frac{e^{-\beta_r}}{2 \cosh \beta_r} K^+(x, y) & \frac{e^{\beta_r}}{2 \cosh \beta_r} K^-(x, y) \end{pmatrix}, \quad (\text{C.15})$$

where

$$K^{\sigma^0}(x, y) = \langle\langle \delta(y - g^{\sigma^0}(x, z)) \rangle\rangle_z. \quad (\text{C.16})$$

We denote with $\Psi(x) = \begin{pmatrix} \psi^+(x) \\ \psi^-(x) \end{pmatrix}$ and $\Phi(x) = \begin{pmatrix} \phi^+(x) \\ \phi^-(x) \end{pmatrix}$ the right and left eigenvectors respectively. It is actually easy to see that at leading order in n the largest eigenvalue is 1 and $\Psi(x) = \begin{pmatrix} 1 \\ 1 \end{pmatrix}$, while $\Phi(x)$ can be computed numerically, by iteratively applying K to any sufficiently well-behaved function, and normalized so that $\int \phi^{+, -}(x) dx = 1$. To linear order in n , the largest eigenvalue $\lambda = 1 + kn$ is found by expanding the Kernel

$$K_n^{\sigma^0}(x, y) \approx \langle\langle \delta(y - g^{\sigma^0}(x, z)) \rangle\rangle_z + n \langle\langle \delta(y - g^{\sigma^0}(x, z)) [-\gamma z - \gamma^2 \sigma^0 + \beta_s + \log(1 + bx)] \rangle\rangle_z \quad (\text{C.17})$$

$$= K_0^{\sigma^0}(x, y) + n \delta K^{\sigma^0}(x, y) \quad (\text{C.18})$$

and leveraging the eigenvalue condition

$$\begin{aligned} k &= \int dx dy \Phi(x) \delta K(x, y) \Psi(y) \\ &= \int dx \phi^+(x) \left(\frac{e^{\beta_r}}{2 \cosh \beta_r} \delta K^+(x) + \frac{e^{-\beta_r}}{2 \cosh \beta_r} \delta K^-(x) \right) \\ &\quad + \int dx \phi^-(x) \left(\frac{e^{-\beta_r}}{2 \cosh \beta_r} \delta K^-(x) + \frac{e^{\beta_r}}{2 \cosh \beta_r} \delta K^+(x) \right) \\ &= \frac{1}{2} \int dx [\phi^+(x) \delta K^+(x) + \phi^-(x) \delta K^-(x)] \end{aligned}$$

where $\delta K^{\sigma^0}(x) = \beta_s - \gamma^2 \sigma^0 + \log(1 + xb)$. Finally, defining $\hat{\phi}^{+, -}(t) := e^t \phi^{+, -}(e^t)$, we obtain

$$k = \frac{[\beta_s - \gamma^2 + \int dt \log(1 + be^t) \hat{\phi}^+(t)] + [\beta_s + \gamma^2 + \int dt \log(1 + be^t) \hat{\phi}^-(t)]}{2}, \quad (\text{C.19})$$

and

$$f_{rs}(t) = \lim_{n \rightarrow 0} \frac{\langle Z^n \rangle - 1}{n} = k. \quad (\text{C.20})$$

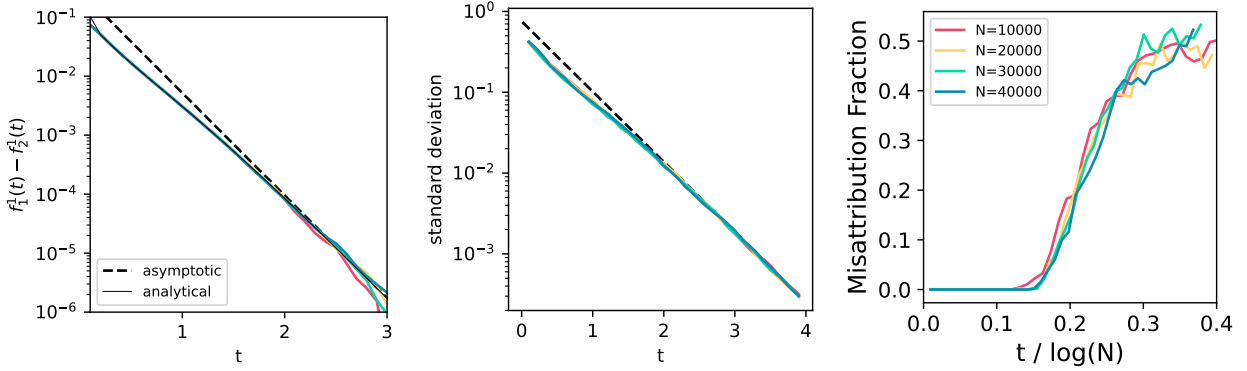


Figure C1: Scaling analysis for a mixture of 1D Ising models with inverse temperature $\beta_1 = 0.5$ and $\beta_2 = 1.0$.

Appendix C.3. Computation of C_{rs}

For inverse temperatures β_r and β_s we define $t_r = \tanh(\beta_r)$, $t_s = \tanh(\beta_s)$. In zero field the magnetization vanishes and the two-point function in the thermodynamic limit is

$$\langle \sigma_i \sigma_j \rangle_r = t_r^{|i-j|}, \quad (\text{C.21})$$

thus the connected correlations are

$$C_{ij}^{(r)} = t_r^{|i-j|}, \quad C_{ij}^{(s)} = t_s^{|i-j|}. \quad (\text{C.22})$$

We therefore have

$$\Delta_{rs} C_{ij} = C_{ij}^{(r)} - C_{ij}^{(s)} = t_r^{|i-j|} - t_s^{|i-j|}. \quad (\text{C.23})$$

The quantity of interest is

$$C_{rs} = \frac{1}{N} \sum_{i,j=1}^N (\Delta_{rs} C_{ij})^2. \quad (\text{C.24})$$

In a periodic chain, for any fixed separation $k \geq 1$ there are $2N$ ordered pairs (i, j) with $|i - j| = k$, while the $k = 0$ term vanishes because $\Delta_{rs} C_{ii} = 0$. Taking the thermodynamic limit $N \rightarrow \infty$, we obtain

$$C_{rs} = 2 \sum_{k=1}^{\infty} (t_r^k - t_s^k)^2. \quad (\text{C.25})$$

Expand the square and write

$$C_{rs} = 2 \left[\sum_{k=1}^{\infty} t_r^{2k} + \sum_{k=1}^{\infty} t_s^{2k} - 2 \sum_{k=1}^{\infty} (t_r t_s)^k \right]. \quad (\text{C.26})$$

Each series is geometric and convergent for $|t_r|, |t_s| < 1$:

$$\sum_{k=1}^{\infty} t_r^{2k} = \frac{t_r^2}{1 - t_r^2}, \quad \sum_{k=1}^{\infty} t_s^{2k} = \frac{t_s^2}{1 - t_s^2}, \quad \sum_{k=1}^{\infty} (t_r t_s)^k = \frac{t_r t_s}{1 - t_r t_s}. \quad (\text{C.27})$$

Therefore the thermodynamic-limit expression for C_{rs} is

$$C_{rs} = 2 \left[\frac{\tanh^2(\beta_r)}{1 - \tanh^2(\beta_r)} + \frac{\tanh^2(\beta_s)}{1 - \tanh^2(\beta_s)} - \frac{2 \tanh(\beta_r) \tanh(\beta_s)}{1 - \tanh(\beta_r) \tanh(\beta_s)} \right]. \quad (\text{C.28})$$

Appendix C.4. Large N

For a mixture of 1D Ising models, we know how to compute analytically the left hand side of Eq. (11), but we do not have an analytical counterpart for the right hand side. In section 5 we described how to estimate speciation times approximating the right-hand side with its asymptotic value, obtained from a Gaussian approximation for large times, derived in Eq. (14)

$$|f_{rr}(t_{rs}) - f_{rs}(t_{rs})| = K \sqrt{\frac{C_{rs}}{2N}} e^{-2t_{rs}}. \quad (\text{C.29})$$

This approximation holds when speciation times are large enough so that the Gaussian approximation is valid, namely for large enough N . Since U-turn experiments are very expensive for large N , in Fig. 3 we limited ourselves to N up to 3200. For this reason, we resorted to the experimental value of the right hand side of Eq. (11) to provide an accurate estimate of speciation times. In this section, we report results for larger N values that account only for the forward process. Nonetheless, they prove that for large times the asymptotic expression for free entropy difference average and variance are correct. In the left panel of Fig. C1 we compare the average free entropy difference for a 2-Ising mixture with inverse temperatures $\beta_1 = 0.5$ and $\beta_2 = 1.0$ obtained numerically with the analytical value and with the asymptotic scaling. In the central panel, we do the same for the right hand side of Eq. (11), only without the analytical value that we did not compute analytically. Finally, in the right panel of Fig. C1, we verify that the scaling of the misattribution fraction coincides with the one of speciation, since rescaling time by $\log N$ all curves collapse.

Appendix C.5. Exact Score

The exact score function can be obtained from

$$S(x; t) = -\frac{x - e^{-t}\langle s \rangle_x}{\Delta_t} \quad (\text{C.30})$$

where the average of s under the tilted measure reads

$$\langle s_i \rangle_x = \int ds s_i P(s | x) = \int ds s_i \frac{P(s, x_t)}{P(x_t)} \quad (\text{C.31})$$

In the Ising mixture case, one has

$$P(s, x_t) = P_0(s) \frac{e^{-\frac{(x-s e^{-t})^2}{2\Delta_t}}}{\sqrt{2\pi\Delta_t}^N} = \frac{1}{\sqrt{2\pi\Delta_t}^N} e^{-\frac{\|x_t - s e^{-t}\|^2}{2\Delta_t}} \left(\sum_r w_r \frac{e^{\beta_r \sum_i s_i \sigma_{i+1}}}{Z_r} \right) \quad (\text{C.32})$$

with $Z_r = 2(2 \cosh \beta_r)^{N-1}$, leading to

$$\langle s_i \rangle_x = \int ds s_i P(s | x) = \frac{\int ds s_i e^{\sum_i \frac{e^{-t}}{\Delta_t} x_i^t s_i} \sum_r w_r \frac{e^{\beta_r \sum_i s_i \sigma_{i+1}}}{Z_r}}{\int ds e^{\sum_i \frac{e^{-t}}{\Delta_t} x_i^t s_i} \sum_r w_r \frac{e^{\beta_r \sum_i s_i \sigma_{i+1}}}{Z_r}}. \quad (\text{C.33})$$

Both the trace in the denominator and the average in the numerator can be computed through the transfer matrix method, for each value of x . For every β_r , the terms in the denominator are standard partition functions

$$B(\beta) = \int ds \frac{e^{\beta \sum_i \sigma_i \sigma_{i+1} + \frac{e^{-t}}{\Delta_t} \sum_i x_i \sigma_i}}{Z(\beta)} = \text{Tr} \prod_{i=1}^N \frac{T_i^\beta}{z_\beta} \quad (\text{C.34})$$

where

$$T_i^\beta = \begin{pmatrix} e^{\beta + \frac{e^{-t}}{\Delta_t} x_i} & e^{-\beta - \frac{e^{-t}}{\Delta_t} x_i} \\ e^{-\beta + \frac{e^{-t}}{\Delta_t} x_i} & e^{\beta - \frac{e^{-t}}{\Delta_t} x_i} \end{pmatrix}$$

and $z_\beta = e^\beta + e^{-\beta}$. Instead, terms in the numerator will have the form

$$A(\beta)_j = \int ds s_j \frac{e^{\beta \sum_i \sigma_i \sigma_{i+1} + \frac{e^{-t}}{\Delta_t} \sum_i x_i \sigma_i}}{Z(\beta)} = \sum_{s_j} s_j \text{Tr} \left(\left(\prod_{i=j}^N \frac{T_i^\beta}{z_\beta} \right) \left(\prod_{i=1}^{j-1} \frac{T_i^\beta}{z_\beta} \right) \right). \quad (\text{C.35})$$

Finally

$$\langle s \rangle_x = \frac{\sum_r w_r A(\beta_r)}{\sum_r w_r B(\beta_r)}. \quad (\text{C.36})$$